Role of steric and electrostatic effects in the short-range order of quasitetrahedral molecular liquids

Sz. Pothoczki,[1,*] A. Ottochian,[1] M. Rovira-Esteva,[1] L. C. Pardo,[1] J. Ll. Tamarit,[1] and G. J. Cuello[2]

[1]*Grup de Caracterització de Materials, Departament de Física i Enginyeria Nuclear, ETSEIB, Universitat Politècnica de Catalunya, Diagonal, 647 08028 Barcelona, Catalonia, Spain*

[2]*Institut Laue Langevin, 6 Rue Jules Horowitz, Boîte Postale 156x, F-38042 Grenoble Cedex 9, France*

(Received 17 September 2011; revised manuscript received 16 November 2011; published 20 January 2012)

The study of how both steric and electrostatic interactions affect the structure of liquids formed by quasitetrahedral molecules has been undertaken in this work. We have studied trichlorobromomethane ($CBrCl_3$) and dibromodichloromethane (CBr_2Cl_2), both displaying a dipole along their C_{3v} and C_{2v} molecular symmetry axes, respectively. The short-range order of the liquid state has been determined using neutron diffraction experiments that were modeled through the reverse Monte Carlo (RMC) technique. To study changes in steric effects due to the distortion of the tetrahedral symmetry, we have compared our results with a previous RMC modeling of carbon tetrachloride (CCl_4). The subtle effects of the dipole in the structure of the liquid have been determined using a set of molecular dynamics simulations with and without atomic partial charges, being the force field validated via comparison with the diffraction data. In a first approximation, neither steric nor electrostatic interactions are able to modify the molecular ordering of a fully tetrahedral liquid such as CCl_4. A more detailed analysis indicates that, although the interaction between dipoles does not have appreciable effects when aligned along the C_{3v} molecular axes, as for the $CBrCl_3$, it enhances the antiparallel orientation of dipoles when it is oriented along the C_{2v} axes, as in the case of CBr_2Cl_2.

DOI: 10.1103/PhysRevB.85.014202 PACS number(s): 61.25.Em, 61.05.F−, 61.20.Ja

I. INTRODUCTION

Molecular disordered systems such as liquids are devoid of ordering only at long length scales. Locally, each molecule tends to minimize the configuration energy relative to its neighbors, giving rise to a short-range ordered structure. This local ordering that does not minimize the energy of the system as a whole but, only locally, has been identified as one of the reasons for the existence of glasses.[1,2] Quantifying the local ordering of a polyatomic molecular liquid from diffraction experiments is not a simple task. The basic problem is that, due to the isotropy of the liquid, diffraction experiments give an average of the distance between molecules. In other words: the subtle spatial short-range order (SRO) of the liquid is collapsed into a one-dimensional pattern or, at best, when enough isotopic substitutions are possible, into as many patterns as contributions from atomic pairs. In any case, molecular orientations must be inferred somehow from a histogram of distances measured in the reciprocal space. To overcome such a problem, two types of computational methods are mainly proposed to study the liquid structure: molecular dynamics (MD) simulations and reverse Monte Carlo (RMC) methods.

In MD simulations, after a force field between the molecules is set, the equations of motion of the system are integrated along a microcanonical path. The information on the structure is calculated by averaging uncorrelated configurations collected along this path. The correctness of the force field is then tested by comparing the obtained structure factor $S(q)$ with the experimental one. The main advantage of this method is that the system by itself reaches the single structure compatible with the given force field and the thermodynamic conditions. The great drawback is that the force field must be known beforehand to describe real data.[3]

The RMC[4,5] method and the empirical potential structure refinement (EPSR)[6,7] are inverse methods that produce structures in real space consistent with experimental data measured in the reciprocal space. Then the structure is analyzed only from the configurations that match the experimental diffraction pattern within its error. The considerable advantage of RMC modeling for molecular liquids is that no knowledge of the system is required beforehand (apart from the density and a reasonable initial molecular structure that will be refined during the process).

In this paper, we have used both self-contained MD and RMC techniques for two reasons, first, because if the short-range order obtained from both of them is the same, it will reinforce the conclusions obtained from the present work and, second, because a lack of a direct comparison between the two methods is found in the literature.

Concerning the intermolecular structure in disordered phases, different methods to characterize the relative orientations of molecules can be found in the literature.[8–13] In this paper, the local molecular ordering is studied with an extensive up-to-date analysis by means of 2D distribution maps already used in previous works.[14–17]

The molecular structure of the halogenomethane derivatives $CCl_xBr_{(4-x)}$ ($x = 0, \ldots, 4$), formed by a central carbon atom and a combination of four chlorine and bromine atoms, is close to a perfect tetrahedron. Moreover, their quasiglobular shape results in a similar phase behavior. They display, on cooling from the liquid, a plastic phase where the molecules can rotate almost freely, but the centers of mass are unable to diffuse away from the equilibrium points of a regular lattice. On further cooling, all of them form also a low-temperature ordered monoclinic phase with the same structure.[18–20] The choice in this work of the trichlorobromomethane $CBrCl_3$ (TCl) and dibromodichloromethane CBr_2Cl_2 (DBr) substances is based on the symmetry properties of their dipolar moments, which are quite similar in magnitude[21] but aligned along their C_{3v} and C_{2v} axes, respectively. These facts make these systems especially suited to study the effects of both steric and electrostatic interactions in tetrahedral molecular liquids.

In order to disentangle the features of the molecular ordering arising from the steric effects or from the electrostatic interaction, two different strategies exploiting the advantages of the two aforementioned methods (MD and RMC) have been adopted. Firstly, we have compared our results with the well-known CCl_4 molecular liquid.[22–27] Due to the fact that the latter has a perfect tetrahedral symmetry, it can be used as a reference system to study the steric effects that arise from the symmetry breaking in the distorted tetrahedral molecules TCl and DBr. Afterwards, the influence of the electrostatic effects is analyzed by a series of two MD simulations: one without electrostatic interactions, the other adding partial charges to the atoms.

The paper is organized as follows: in Sec. II, the details of the neutron diffraction experiments, RMC and MD simulations, and their consistence are exposed. In Sec. III, the SRO analyses for TCl, DBr, and their comparison with the reference system (CCl_4) are conducted using a bivariate angular analysis. We will first analyze the relative position of two molecules and then their relative orientations. Finally, we summarize the main results comparing the two compounds with the reference system.

II. EXPERIMENTAL AND COMPUTATIONAL DETAILS

A. Experimental details

Samples of TCl ($CBrCl_3$) and DBr (CBr_2Cl_2) were obtained from Sigma-Aldrich (St. Louis, USA) and Acros Organics (Geel, Belgium) with a purity of 99+% and 99%, respectively. Since the measured melting points agreed well with the ones reported in the bibliography, no further purification was performed. Experiments were carried out at the Institute Laue Langevin (Grenoble, France). In the case of DBr, the D4C diffractometer was used with a wavelength of $\lambda = 0.5$ Å, and for TCl, the D1B diffractometer with $\lambda = 1.28$ Å. Empty cryostat, empty sample holder, and an absorbing sample were also measured to perform corrections on the data due to the sample environment contributions to the pattern, and a cylindrical vanadium rod was also measured in order to normalize data and correct the detector efficiency. Self-absorption corrections were performed using the Paalman and Pings approach. As in previous works,[15–17] all the aforementioned effects, together with multiple scattering corrections, were performed using the software CORRECT,[28] and inelastic corrections were additionally carried out by subtracting a polynomial expansion in powers of q^2.

B. Reverse Monte Carlo modeling: computational details

Neutron diffraction experiments were interpreted by means of RMC computer modeling, which constructs large structural models that are consistent with experimental results within the experimental errors. The total scattering structure factor was modeled considering both intra- and intermolecular parts. A detailed description of RMC modeling can be found in Refs. 4, 5, 29, and 30, and therefore, here, we provide only the relevant points.

The initial configurations contained 2000 randomly oriented molecules in cubic boxes with periodic boundary conditions. The box lengths were 68.998 Å for TCl and 69.282 Å for DBr, corresponding to atomic densities of 0.03044 $Å^{-3}$ for TCl and 0.03007 $Å^{-3}$ for DBr, chosen according to the experimental densities.[18,20] The molecular units are held together by fixed neighbor constraints (*fnc*), which allow bond lengths to fluctuate within predefined tolerances. This approach proved to be very useful for other molecular liquids.[31,32] The basic parameters of the simulations such as *fnc* limits and intermolecular minimum atom-atom (cutoff) distances can be found in Table I.

TABLE I. Characteristics of the molecular computer models used in the RMC modeling (*fnc*: fixed neighbor constraints corresponding to the tolerances of intramolecular bond lengths; r_{cutoff}: intermolecular closest approaches between atoms).

	TCl ($CBrCl_3$)		DBr (CBr_2Cl_2)	
	fnc (Å)	r_{cutoff} (Å)	*fnc* (Å)	r_{cutoff} (Å)
C-C		3.5		3.5
C-Br	1.83–2.07	2.5	1.83–2.03	2.5
C-Cl	1.63–1.90	2.5	1.65–1.85	2.5
Br-Br		3.0	3.083–3.283	3.0
Cl-Br	2.89–3.17	2.9	2.87–3.07	2.9
Cl-Cl	2.77–3.03	2.7	2.8–3.1	2.7
	Angle (°)		Angle (°)	
Cl-C-Cl	110 ± 8		112.5 ± 5	
Br-C-Cl	110 ± 8		107.5 ± 5	
Br-C-Br			112.5 ± 5	

All calculations were run for several million accepted moves, where the ratio of accepted/rejected moves varied between 1:3 and 1:10, i.e. typically several thousand moves were accepted per atom. The RMC modeling of CCl_4 has been taken from previous work.[25,27]

C. Molecular dynamics simulations: computational details

In the MD simulations, we considered for both TCl and DBr liquids models without and with atomic partial charges. We studied therefore four liquid systems of $N = 864$ molecules (256 when the electrostatic interaction is included for TCl) enclosed in a cubic box with periodic boundary conditions. The box dimensions are chosen in order to reproduce the same density of the experimental samples. Since for the moment we neglect internal motions, the models consist of rigid molecules. The bonds and the intramolecular angles, detailed in Table II, were provided by fitting the high-q region of the total scattering structure factor of the neutron diffraction using a Bayesian fit scheme.[16,33] This ensures the best coincidence of the structure function $S(q)$ at high q between the MD model and the

TABLE II. Bond lengths and angles for the rigid molecule model of TCl and DBr obtained by the high-q fit of the diffractogram.

	TCl ($CBrCl_3$)	DBr (CBr_2Cl_2)
C-Br	1.949 Å	1.953 Å
C-Cl	1.760 Å	1.775 Å
Cl-C-Cl	108.5°	109.2°
Br-C-Cl	110.4°	109.2°
Br-C-Br		111.0°

experiments; in other words, it ensures the molecular geometry is realistic. The matching between the values that provides a good description of the data using the RMC modeling (Table I) and those arising from the high-q fit (Table II) is excellent. Moreover, with regard to the molecular geometry, the obtained values for the angles yield that TCl and DBr are indeed quasitetrahedral molecules (tetrahedral angle is around 109.5°).

The corresponding geometrical constraints were satisfied with the SHAKE algorithm[34] with a relative accuracy of 10^{-6}. For the intermolecular interaction, the Optimized Potentials for Liquid Simulations parameters were used, and a spherical truncation scheme between molecular centers was taken with a cutoff value of 12 Å. When electrostatic forces are introduced, the Ewald summation method has been used, with the convergence parameter $\alpha \sim 13/L$ and $k_{\max} = 14$. The equations of motion have been integrated with the Leapfrog algorithm and a time step of 1 fs. Molecules were initially placed in an Face-centered cubic lattice with random orientation for all systems, and then the system was equilibrated at 450 K in the NVT ensemble. Then successive NVT equilibrations using Berendsen method with a relaxation time of $t = 0.01$ ps were applied for a time of 20 ps at 300 and 273 K for TCl and DBr, respectively. A production run was performed in order to obtain at least 25 independent configurations. We considered independent two configurations if the elapsed time between them is 0.1τ, where τ is the relaxation time of the orientational self-correlation function.

D. Consistency with experiments

Figure 1 shows the total scattering structure factors of TCl and DBr obtained from the experiment together with those obtained from RMC and MD techniques. The agreement with the experiment is nearly perfect for both liquids and both techniques, especially for the RMC modeling. In the high-q region, the good agreement of RMC simulation suggests that the molecular structures defined by the *fnc*s are appropriate for these liquids. Concerning the intramolecular structure, the tetrahedral angles arising from RMC (Table I) and MD (Table II) do not differ significantly from each other. This ascertains the quasitetrahedral geometry of the molecules that can be seen in Fig 3, where the molecules have been depicted following the intramolecular parameters of Table II.

III. RESULTS AND DISCUSSIONS

A. Positional ordering

The local ordering analysis of the molecules in the liquid phase of TCl and DBr has been restricted to the closest molecules because, as shown in Ref. 15, they fully determine the position and orientation of successive molecular shells. However, as it will be seen, due to the quasitetrahedral symmetry of the molecules, it will be possible to find this first molecule at four different positions. In other words, the first molecule might be placed in any of the four positions imposed by the quasitetrahedral symmetry of the molecules with a probability $P = 0.25$. We consider therefore only the molecules up to a distance r_1 defined by the following condition:

$$\mathrm{MCN_{CC}} = 4\pi\rho_0 \int_0^{r_1} g_{\mathrm{CC}}(r)\, r^2 dr = 1 \qquad (1)$$

where $\mathrm{MCN_{CC}}$ is the carbon-carbon molecular coordination number, ρ_0 is the molecular number density (in $\mathrm{Å}^{-3}$ units), and $g_{\mathrm{CC}}(r)$ is the carbon-carbon radial distribution function. As seen in Fig. 2, the $g_{\mathrm{CC}}(r)$ values obtained for TCl, DBr, and CCl_4 using the RMC technique are very similar. No big changes with respect to CCl_4 are thus expected to arise in the short-range molecular order from the tetrahedral symmetry breaking in TCl and DBr. Concerning the $g_{\mathrm{CC}}(r)$ obtained by MD [Figs. 2(b) and 2(c)], the electrostatic effects seem to be negligible for TCl since no significant change is seen adding or not partial charges to the molecules in the simulation. On the contrary, atomic partial charges in DBr impose a more marked structure in $g_{\mathrm{CC}}(r)$ with higher peaks and a slightly different packing distance. Its origin will be explained later together with the orientational ordering features.

The probability of the relative position between two molecules can be fully determined by the 3D function $g_{\mathrm{CC}}[r,\cos(\theta),\varphi]$, where r is the distance between carbon atoms of the molecules, φ is the equatorial angle, and θ is the azimuthal angle of the vector joining two carbon atoms. In order to define the azimuthal θ and equatorial φ angles for a given reference molecule, a polar frame must be set taking into account the molecular symmetry.[14,16,17]

For TCl, the Z axis lies along the C_{3v} symmetry axis, i.e. the C-Br vector, which is parallel to its dipolar moment, while

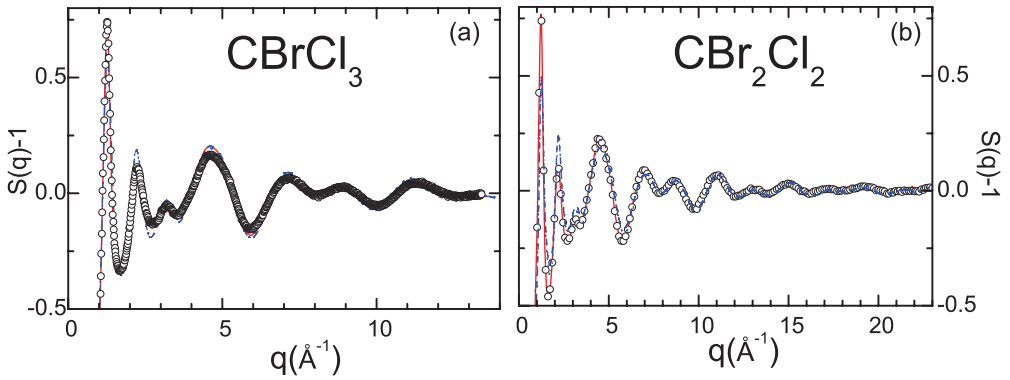

FIG. 1. (Color online) Total scattering structure factors for (a) liquid TCl and (b) DBr. Circles: experimental data; red solid lines: RMC; blue dashed lines: MD simulation.

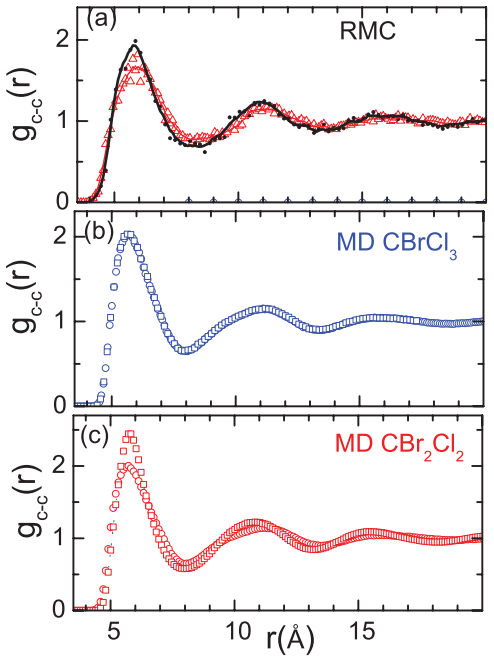

FIG. 2. (Color online) (a) Carbon-carbon partial radial distribution function for TCl (circles), for DBr (triangles), and for CCl_4 (solid line) from the analysis of RMC configurations. The results from MD simulation switching on (squares) and off (circles) the electrostatic interaction, respectively, are also shown in (b) for TCl and (c) for DBr.

the origin of angle φ lies in one of the Br-C-Cl molecular planes [see Fig. 3(a)]. Similarly, for the DBr molecule, the Z axis is set along its C_{2v} symmetry axis, i.e. parallel to the bisecting vector between the two C-Br vectors which, as in TCl, is also parallel to the dipolar moment of the molecule. The φ equatorial angle origin is set in this case in the Br-C-Br plane [see Fig. 3(b)]. For the sake of comparison between the three molecular liquids, the CCl_4 reference system has been defined both along its C_{3v} axis, as in TCl, and along its C_{2v} axis, as in DBr.

The positional molecular ordering for each system is described through a 2D probability map (Figs. 4 and 5) given by the bivariate analysis of φ and $\cos(\theta)$. The probability related to the azimuthal angle θ is calculated using the cosine of the angle instead of the angle. To meet the requirement that an isotropic distribution should lead to a flat probability map, P has been normalized to the map area. Four calculations have been performed for each compound (TCl and DBr): (a)

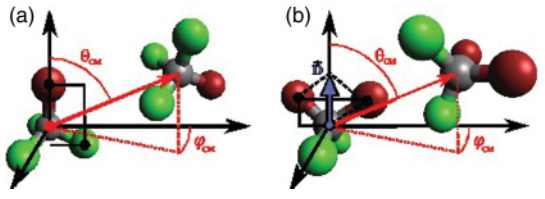

FIG. 3. (Color online) Arbitrary arrangements of two (a) TCl and (b) DBr molecules showing the axes and θ and φ angle definitions used to determine the molecular position. Green (light gray), red (dark gray), and gray spheres represent the Cl, Br, and C atoms, respectively.

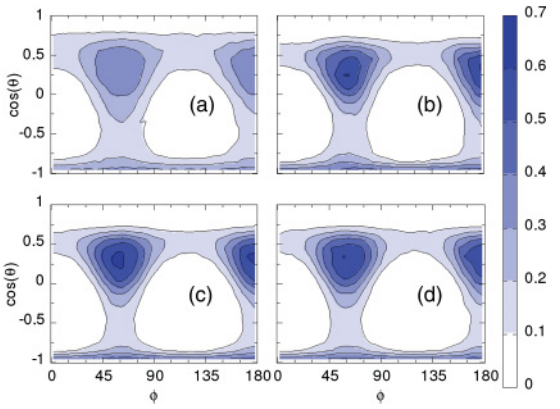

FIG. 4. (Color online) Positional ordering for studied liquids (TCl) with C_{3v} symmetry. (a) Reference system (RMC modelization of CCl_4), (b) RMC modeling, (c) MD simulation without charges, and (d) MD simulation with charges.

reference system CCl_4 obtained from RMC modelization using the symmetry axis of the molecule studied: C_{3v} in the case of TCl and C_{2v} in the case of DBr, (b) RMC modeling of the studied system, (c) MD simulation without partial charges, and (d) MD simulation with partial charges. As it is seen in Figs. 4 and 5, results arising from the RMC model (b) and the MD simulation (d) are virtually the same, thus assuring the robustness of the obtained positional orderings.

In order to analyze the positional maps of Figs. 4 and 5, we present in Table III the coordinates where the spots arising from the relative positions $[\varphi,\cos(\theta)]$ should appear, assuming that the carbon atom of the neighbor molecule sits in front of the tetrahedral faces of the reference one and that the molecule has full tetrahedral symmetry as in CCl_4, i.e. that there is a carbon atom in front of all four tetrahedron faces. The calculations were performed using the two axes definitions of Fig. 3, thus setting the Z axis along the C_{3v} and C_{2v} symmetry axes of the tetrahedron. In the first case, a carbon atom of a neighbor molecule placed in front of the bottom face of the tetrahedron [see Fig. 3(a)], that is $\theta = 180^\circ$, would give a contribution to the 2D positional map at $\cos(\theta) = -1$, and φ would be undetermined because it corresponds with the

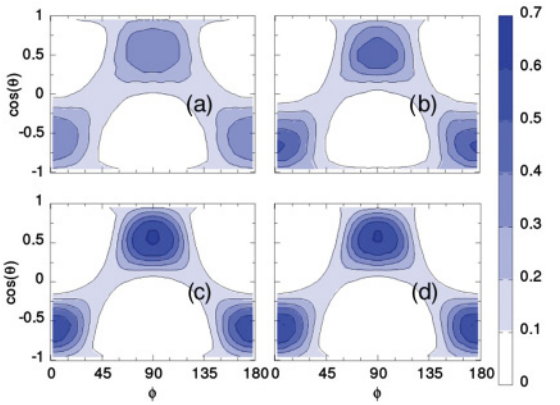

FIG. 5. (Color online) Positional ordering for studied liquids (DBr) with C_{2v} symmetry. (a) Reference system (RMC modelization of CCl_4), (b) RMC model, (c) MD simulation without charges, and (d) MD simulation with charges.

TABLE III. Coordinates of the spots expected to appear in the 2D probability maps describing the relative position of two molecules, if carbon atoms of a neighbor molecule sit on the face of the tetrahedron of a reference molecule. Calculations have been performed in the frames of reference parallel to both the C_{3v} and C_{2v} axes of the tetrahedron (see Figure 3). For molecules located in the poles, the φ coordinate is undetermined.

Symmetry axis	Figure number	φ	$\cos(\theta)$	θ
C_{3v}	Fig. 4	Undetermined	-1	180.0°
		60°, 180°, 300°	$+0.33$	70.5°
C_{2v}	Fig. 5	0°, 180°	-0.58	125.3°
		90°, 270°	$+0.58$	54.7°

pole of the coordinate system. Molecular symmetry, however, imposes that the neighbor molecules are also found in front of the three upper faces of the tetrahedron, with an azimuthal angle of $\theta = 70.5°$. These are the positions corresponding to the [φ,cos(θ)] pairs (60°,0.33), (180°,0.33), and (300°,0.33), the last being equivalent to (60°,0.33) in the probability map due to XZ symmetry.

The [φ,cos(θ)] pairs obtained by placing the Z vector in the C_{2v} molecular axis are calculated in a similar way. In this case, the spots appear at the [φ,cos(θ)] pairs (0°,-0.58) and (180°,-0.58) and also at (90°,$+0.58$), equivalent to (270°,$+0.58$) due to the XZ symmetry. The first two pairs correspond to neighbor molecules located at $\theta = 125.3°$ in front of the lower faces formed by two Cl and one Br atoms, and the last two correspond to molecules located at $\theta = 54.7°$ in front of the upper faces formed by one Cl and two Br atoms. Note that changing the frame of reference in CCl_4 changes the position and the shape of the probability spots in the positional maps, but not their meaning. In the case of TCl, the change of the spot shape is extreme because molecules sitting in the lower face of the molecule are to be seen as a large spot without a well-defined equatorial angle (in fact, this happens whenever trying to perform a projection from spherical coordinates into a 2D map).

Concerning CCl_4, since only the spots calculated in Table III appear in Figs. 4(a) and 5(a), we conclude that the preferred relative positions of the two closest molecules are the neighboring molecules being arranged in front of the respective tetrahedron faces of the reference molecule (see Table III) in concordance with previous works.[15]

In order to study how the distortion of the tetrahedral symmetry affects the liquid structure of TCl and DBr, RMC results for both liquids [Figs. 4(b) and 5(b)] have been compared with the reference system CCl_4 [Figs. 4(a) and 5(a)]. It can be seen that this distortion seems to have no effect in the relative position of two neighbor molecules, given the similarity of the maps. In other words, TCl and DBr behave as fully tetrahedral liquids concerning the relative position of two neighboring molecules. Moreover, the positional maps of TCl and DBr obtained from the MD simulations performed without and with partial charges [Figs. 4(c) and 5(c) and Figs. 4(d) and 5(d), respectively] both yield a high similarity to that obtained for the CCl_4 [Figs. 4(a) and 5(a)]. This shows that the electrostatic interaction plays no relevant role in the relative position of neighbor molecules, neither in TCl nor in DBr, and indicates also that the differences between the $g_{CC}(r)$ from the two MD simulations for DBr [see Fig. 3(a)] arise not from the positional ordering but from their relative orientation (see next section).

B. Orientational ordering

The orientational ordering is usually studied simply taking into account an angle between two characteristic vectors of a reference molecule and its first neighbors. Typically, only the probability distribution of the cosine of that angle is calculated in the literature. However, this unidimensional distribution hides the fact that molecules in different positions might have different orientations. In order to identify the position of the molecules with a given orientation, the probability distribution has been calculated as a function of an angle characterizing molecular orientation, α, and an angle related to the relative position, the azimuthal angle θ, thus generating a 2D probability map[10] (Figs. 6 and 7). As explained before, probabilities are calculated using the cosines of the angles when necessary so that isotropic distributions lead to flat probability maps. As in the case of the molecular position determination, four types of calculations have been performed for each liquid (TCl and DBr): (a) reference system CCl_4, obtained with the same method as in Figs. 4 and 5, (b) RMC modeling of the studied system, (c) MD simulation without partial charges, and (d) MD simulation with partial charges. It is worth pointing out that the good agreement between the RMC [Figs. 6(b) and 7(b)] and the MD simulations [Figs. 6(c) and 7(c) and Figs. 6(d) and 7(d)] ascertains that also the orientational ordering analysis for both TCl and DBr is grounded on a solid base.

First of all, we should recall that the x and y axes are related to relative orientation and position of two molecules, respectively. Therefore, concerning the position, the lower horizontal bands in Fig. 6 in the probability maps correspond to orientations of the neighbor molecule located in front of the bottom face of the tetrahedron, and the upper bands correspond to the orientations of neighbors located in front of the three upper faces. On the other hand, Fig. 7 shows in the higher bands

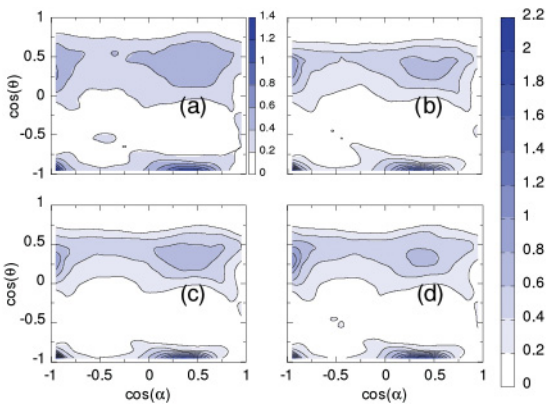

FIG. 6. (Color online) Orientational ordering for studied liquids with C_{3v} (TCl) symmetry. (a) Reference system (RMC modeling of CCl_4), (b) RMC model, (c) MD simulation without charges, and (d) MD simulation with charges.

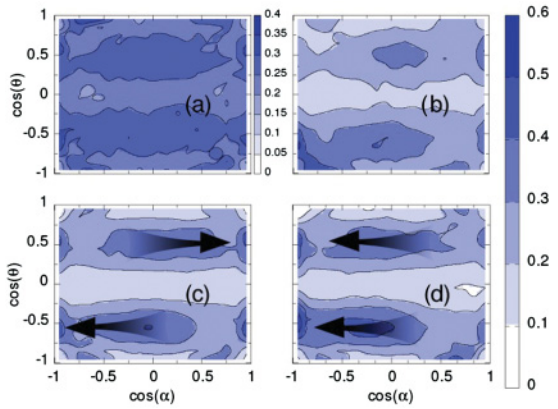

FIG. 7. (Color online) Orientational ordering for studied liquids with C_{2v} (DBr) symmetry. (a) Reference system (RMC modeling of CCl_4), (b) RMC model, (c) MD simulation without charges, and (d) MD simulation with charges. Arrows in (c) and (d) indicate, respectively, the steric and the steric plus electrostatic effect on the molecular ordering.

the orientation of the neighbors in front of the two upper faces of the tetrahedron and in the bottom bands of the molecules located in front of the two bottom faces.

At a first stage, we will only focus on two relative molecular orientations to simplify our discussion: the parallel configuration and the antiparallel one. The orientation of two molecules is parallel when the characteristic vectors chosen to describe the relative orientation of two molecules (the C_{3v} and C_{2v} symmetry axis for CCl_4 and the dipolar moment for molecules DBr and TCl) are parallel, giving a trivial contribution at $\cos(\alpha) = 1$ (spots appearing at the right edge of the graphs in Figs. 6 and 7). In the case of an antiparallel ordering, the spot in the probability map should be located at $\cos(\alpha) = -1$ (at the left edge of the same graphs). However, due to molecular symmetry and the degeneration of the reference frame definition, additional orientational spots can appear for the same position of a neighbor molecule, i.e. for the same value of $\cos(\theta)$.

In the case of two fully tetrahedral CCl_4 molecules with one C-Cl vector (the C_{3v} molecular axis) oriented antiparallel to each other, the trivial contribution will be found at $\cos(\alpha) = -1$ in Fig. 6(a). The contributions at $\cos(\alpha) = 0.33$ are given by the angles between the remaining three C-Cl vectors of each molecule that, for symmetry reasons, are the only compatible with the closest packing of a tetrahedral molecule. On the other hand, if the same molecular ordering is evaluated, taking into account a C_{2v} molecular axis as in Fig. 7(a) in addition to the contribution at $\cos(\alpha) = -1$, nontrivial spots will appear at $\cos(\alpha) = 1$ and $\cos(\alpha) = 0$. The calculations for the pairs $[\cos(\alpha),\cos(\theta)]$, taking into account the orientations using the C_{2v} and C_{3v} tetrahedron axes, are gathered in Table IV. As it can be seen, these spots are not enough to distinguish between parallel and antiparallel configurations in the case of C_{2v} symmetry. However, the calculated spots in Table IV are compatible with the antiparallel configuration [see Figs. 6(a) and 7(a)], in agreement with previous results on CCl_4.[15] Concerning TCl and DBr, the orientational map also corresponds to the antiparallel configuration, regardless of whether they are distorted tetrahedra and do not possess the C_{3v} or C_{2v} symmetry axes, respectively. This yields to the conclusion that, in a first approximation, neither steric nor electrostatic effects substantially change the short-range ordering of the DBr and TCl nearly tetrahedral molecules, neither the position nor the orientation of neighboring molecules.

In Fig. 8, we have depicted the most probable configuration of the first neighbor for both liquids TCl and DBr obtained from the information of the probability maps in Figs. 4–7. Reference molecules have been oriented along their C_{3v} and C_{2v} axes, respectively, as in Fig. 3. As seen in Figs. 4 and 5, first neighbors can be in front of any of the four faces of the tetrahedron, but for the sake of clarity, only the molecule in front of one of the faces has been depicted. Concerning the orientation, we show in Fig. 8 only the configuration corresponding to the spots at $\cos(\alpha) = -1$ in Figs. 6 and 7 because this probability is slightly higher for DBr. The other configurations can be obtained from successive rotations around the axes of their associated tetrahedra, generating the large spots at $\cos(\alpha) \approx 0$.

A more detailed analysis of the relative molecular orientation in TCl and DBr can be carried out, taking into account that the obtained probability maps constitute a quantitative way to determine molecular orientation. Molecules with an unlikely arrangement will hardly be observed and will prefer to have the relative position and orientation associated to high-probability regions. Therefore, the low-probability regions might be seen

TABLE IV. Spots expected to appear in the probability map P(cos α,cos θ) when the parallel or antiparallel orientation is assumed, being the molecules located in front of the faces of the reference molecule. In addition to the trivial $\cos(\alpha) = \pm 1$ contributions (bold in the table), the spots that would appear just due to assuming a fully tetrahedral symmetry, as in the case of CCl_4, have also been calculated.

Symmetry	Orientation	(cos α,cos θ)	(α,θ)
C_{3v}	Parallel	(1,−1) (1,−0.33)	(0°,180°) (0°,109.5°)
(Fig. 6)	Antiparallel	(−0.33,−1) (−0.33,0.33)	(109.5°,180°) (−70.5°,70.5°)
		(−1,−1) (−1,−0.33)	(180°,180°) (180°,109.5°)
		(0.33,−1) (0.33,0.33)	(70.5°,180°) (70.5°,70.5°)
C_{2v}	Parallel	(1,±0.58)	(0°,125.3°) (0°,54.7°)
(Fig. 7)	Antiparallel	(0,±0.58)	(90°,125.3°)(90°,54.7°)
		(−1,±0.58)	(180°,125.3°) (180°,54.7°)
		(−1,±0.58)	(180°,125.3°) (180°,54.7)
		(0,±0.58)	(90°,125.3°) (90°,54.7°)
		(1,±0.58)	(0°,125.3°) (0°,54.7°)

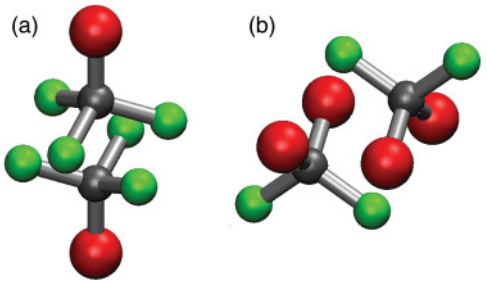

FIG. 8. (Color online) Most probable configuration for (a) TCl and (b) DBr molecular pairs obtained from the probability maps of Figs. 4, 5, 6, and 7. TCl and DBr molecules are oriented along their C_{3v} and C_{2v} axes according to the axis definition of Fig. 3.

as barriers between the molecular configurations described by the high-probability regions. The maximum probability value in each map, P_{max}, is thus related with the height of such barriers and will give us information about how strong a certain molecular ordering is defined. As it can be seen in Figs. 6 and 7, the P_{max} value of CCl_4 is smaller than that of TCl and DBr, respectively. Since this difference is the same for all MD simulations, regardless of whether partial charges are added or not to the atoms, this fact has to be related with the steric effects produced by the loss of tetrahedral symmetry that imposes a more restricted orientation of the neighbor molecules.

Taking into account this relation between a high value of P_{max} and a more defined orientation of a neighboring molecule, some general features concerning the molecular reorientation based on Figs. 6 and 7 should be highlighted. In the foregoing discussion, we will assume that both TCl and DBr are perfect tetrahedra. For example, when referring to a rotation about the C_{3v} symmetry axis of DBr, it will implicitly mean that we assume for that molecule a perfect tetrahedral symmetry and that the rotation is done around a vector going from the central carbon to a Cl or Br atom. When calculations are made taking into account C_{2v} symmetry as in Fig. 7, the probability map appears more smeared out than the one calculated for the C_{3v} molecular symmetry (see Fig. 6). As aforementioned, this feature might be quantified by the maximum of the color scale P_{max}. For the CCl_4 molecule, P_{max} decreases from 1.4 in Fig. 6 to 0.4 in Fig. 7, this decrease is more extreme when TCl (P_{max} = 2.2) is compared with DBr (P_{max} = 0.6). It clearly emerges then that, by modifying the frame of reference from a C_{3v}- to a C_{2v}-oriented axis [Figs. 3(a) and 3(b), respectively], the height of the orientational barrier that a molecule must overcome to change the relative orientation with respect to the neighbor molecule around the axes is decreased, thus the C_{3v} axis being stiffer than the C_{2v} axis.

To explain this fact, it should be noted that rotations that leave the C_{3v} axis unchanged are precisely those around the C_{3v} axis, and these rotations will be responsible for changes in the orientation of the C_{2v} molecular axis. Therefore, the higher value of P_{max} of the orientational map calculated using the C_{3v} axis (Fig. 6), compared to that obtained using the C_{2v} axis (Fig. 7), evidences that the molecular reorientations around the C_{3v} axis (which leave this axis unchanged) are more probable than those around a C_{2v} axis. Moreover, since the probability scale in Figs. 6 and 7 is unchanged by adding or not partial charges, we conclude that the stiffness of the C_{3v} axis is mainly determined by steric effects.

To prove this statement, a simple calculation of the configuration energy profile is shown in Fig. 9 for two neighboring molecules: the first fixed and the other rotating along its C_{3v} and C_{2v} axes, assuming as aforementioned a fully tetrahedral symmetry for the molecules. For both TCl and DBr, the starting relative orientation is energetically the most stable. For both compounds, the energy barriers are much higher for rotations around the C_{2v} axes, which imply a displacement of the C_{3v} axes, than for those around the C_{3v} axes, which leave these axes unchanged, as it is revealed by Fig. 9, in agreement with the conclusion obtained directly from the orientational maps.

Concerning the influence of electrostatic forces in the molecular ordering of TCl, we have compared the orientational maps without and with electrostatic interactions [Figs. 6(c) and 6(d), respectively]. Since the probability maps are almost identical for TCl, we conclude that electrostatic effects do not affect the molecular ordering in this compound. On the other hand, the DBr case is slightly different. The central spots around $[\cos(\alpha),\cos(\theta)] = (0,\pm 0.58)$ are symmetric for CCl_4, whereas in DBr, they become slightly asymmetric. If no partial charges are added to the molecule, a neighbor at positive $\cos(\theta)$ prefers to orient the dipole toward positive values of $\cos(\alpha)$, and at negative $\cos(\theta)$ towards negative values of $\cos(\alpha)$ [see the arrows in Fig. 7(c)]. The reason why changes on the dipole orientation are seen in DBr and not in TCl is because, in the

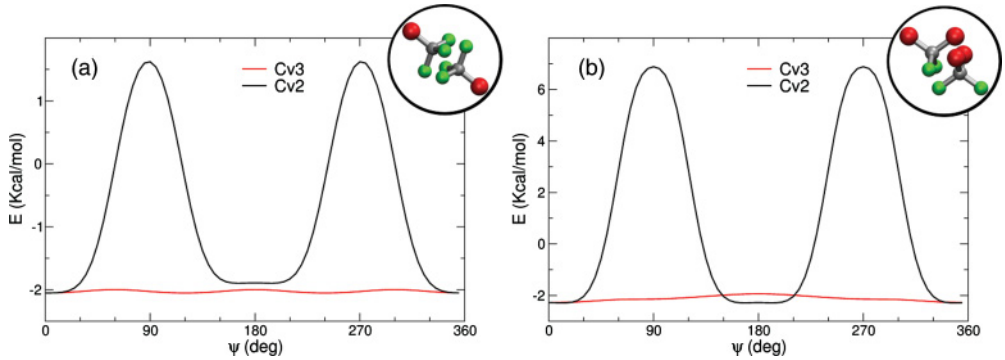

FIG. 9. (Color online) Energy for a dimer formed by the two closest molecules of (a) TCl and (b) DBr as a function of the angle rotated around their C_{2v} axes and around their C_{3v} axes, assuming that both molecules are perfect tetrahedra. Insets show the most stable configuration, chosen as starting configuration for the rotation along C_{3v} and C_{2v} axes, respectively.

first case, the dipole is oriented along the C_{2v} axis that is more mobile than the dipole of TCl oriented along its C_{3v} axis.

To understand this point, we must recall some geometrical facts. The distance from the central carbon to the chlorine atom, $d_{CCl} = 1.775$ Å, is smaller than that to the bromine atom, $d_{CBr} = 1.953$ Å. Therefore, since the Z axis is oriented towards the bromine atoms, the molecule is bulkier upwards $[\cos(\theta) > 0]$ than downwards $[\cos(\theta) < 0]$. The molecular shape of DBr induces thus the neighbors to move in such a direction that the empty space between molecules is minimized. To accomplish this requirement, molecules in the upper part tilt aside of the molecular z axis, and those in the lower tilt inside the z axis. This is seen in Fig. 7(c) as a displacement of the central spot located around $\cos(\theta) = 0.58$ towards larger values of $\cos(\alpha)$ and in the opposite direction for spots located around $\cos(\theta) = -0.58$ [see the arrows in Fig. 7(c)]. So in DBr, the steric effect promotes the parallel or the antiparallel orientation of the C_{2v} axis depending on the relative position of the neighbor molecule.

The electrostatic interaction, on the contrary, tends to orient dipoles in an antiparallel direction to minimize the electrostatic energy. This can be seen when comparing the maps obtained using the MD simulations without and with the partial charges of the molecule [cf. Figs. 7(c) and 7(d), respectively], where the large central spots tend to move towards negative values of $\cos(\alpha)$, irrespective of their position, i.e. irrespective of the sign of $\cos(\theta)$ [see arrows in Fig. 7(d)], when the electrostatic interaction is added. The orientation of two molecules in DBr depends therefore on both steric and electrostatic effect, and their effects are balanced or reinforced depending on the molecular position.

IV. CONCLUSIONS

Reverse Monte Carlo modeling of neutron diffraction measurements has been performed to investigate the intermolecular structure of $CBrCl_3$ and CBr_2Cl_2 liquids composed by slightly distorted tetrahedral molecules. Simultaneously, molecular dynamics simulations have been carried out to study the role of electrostatic interactions in these systems. We provide a comparison with a reference system (CCl_4) to highlight the influence of the steric effects in the short-range order. Our results concerning both mutual position and orientation of molecules are validated by the excellent agreement between the measurements and the simulations (using RMC and MD). Once the robustness of the obtained short-range ordering of molecules is assessed, three sets of conclusions concerning relative position and orientation of molecules and concerning molecular reorientations result.

First of all, as seen when TCl and DBr molecular arrangements in the liquid phase are compared with that of CCl_4, neither steric nor electrostatic interactions produce a change of the relative position of two neighboring molecules with respect to the reference tetrahedral molecule CCl_4 (see Figs. 4 and 5). This statement is supported by the fact that switching on and off the electrostatic forces in the MD simulations of the liquid TCl and DBr does not change their position distributions with respect to liquid CCl_4.

Concerning the relative orientation of two molecules (Figs. 6 and 7), all the spots present on CCl_4 appear as well on both polar molecules, DBr and TCl. Therefore, steric and electrostatic effects are not able to avoid any of the molecular orientations present in CCl_4. A more detailed analysis, though, allows us to detect some differences between TCl and DBr:

In the case of TCl, no appreciable change in any of the studied cases has been seen in comparison with CCl_4. Together with the previous result on the relative position, we can conclude that, in TCl, none of the effects, steric or electrostatic, change the short-range order from that of a fully tetrahedral molecule such as CCl_4.

In contrast, the relative orientation of two molecules shows some differences in the case of DBr. For this compound, the balance between two competing effects determines the molecular ordering. Steric effects force neighbors to reorient, optimizing the molecular packing. This reorientation takes place in opposite directions for each molecule depending on its position due to the molecular asymmetry [see the arrows in Fig. 7(c)]. The electrostatic interactions, on the other hand, tend to orient the molecular dipoles antiparallel, irrespective of their position [see the arrows on Fig. 7(d)]. Therefore, electrostatic and steric effects either reinforce each other or compete depending on the relative molecular position, thus determining the molecular orientation. Finally, the probability maps related to the molecular orientation (Figs. 6 and 7) yield the conclusion that, due to steric effects, movement of the C_{3v} axis in quasitetrahedral molecules is more restricted than the movement of the C_{2v} axis. Two consequences can be drawn from this fact. First of all, the higher mobility of C_{2v} axis causes that electrostatic effects are clearer when the dipole is oriented parallel to this axis, as it happens in DBr. On the other hand, since movements of the C_{3v} axis are more constrained than those of C_{2v}, rotations are more probable around the C_{3v} axis. This conclusion is confirmed by a calculation of the energy barriers that molecules must overcome when rotating around these two molecular axes.

ACKNOWLEDGMENTS

This paper was supported by the Spanish Ministry of Science and Innovation (MICINN) Grant FIS2008-00837 and by the Government of Catalonia (2008SGR-1251). Two of the authors (AO and SzP) acknowledge the postdoctoral fellowships of the Departament de Fisica i Enginyeria Nuclear and the Universitat Politècnica de Catalunya, respectively.

*Univ. Pol. de Cat., Dept. de Fisica i Eng. Nuc., Escola Tecnica Superior d'Enginyeria, Industrial de Barcelona (ETSEIB), Grp of Char. of Mat., Diag. 647 (planta 11), Barcelona, Catalonia, Spain; szilvia.pothoczki@upc.edu

[1]H. Tanaka, J. Chem. Phys. **111**, 3163 (1999).
[2]H. Tanaka, Phys. Rev. E **62**, 6968 (2000).
[3]M. P. Allen and D. Tildesley, *Computer Simulation of Liquids* (Clarendon Press, Oxford, 1987).
[4]R. L. McGreevy and L. Pusztai, Mol. Simul. **1**, 359 (1988).
[5]R. L. McGreevy, J. Phys. Cond. Matter **13**, R877 (2001).

[6]A. K. Soper, Chem. Phys. **202**, 295 (1996).
[7]A. K. Soper, Phys. Rev. B **72**, 104204 (2005).
[8]I. M. Svishchev and P. G. Kusalik, Physica A **192**, 628 (1993).
[9]I. M. Svishchev and P. G. Kusalik, J. Chem. Phys. **99**, 3049 (1993).
[10]P. Jedlovszky, Á. Vincze, and G. Horvai, Phys. Chem. Chem. Phys. **6**, 1874 (2004).
[11]R. Rey, J. Chem. Phys. **129**, 224509 (2008).
[12]L. Temleitner, L. Pusztai, Y. Akahama, H. Kawamura, S. Kohara, Y. Ohishi, and M. Takata, Phys. Rev. B **78**, 014205 (2008).
[13]S. Imberti and D. T. Bowron, J. Phys. Condens. Matter **22**, 404212 (2010).
[14]M. Rovira-Esteva, L. C. Pardo, J. Ll. Tamarit, N. Veglio, and F. J. Bermejo, *Metastable Systems Under Pressure Book Series: NATO Science for Peace and Security Series A-Chemistry and Biology*, edited by S. Rzoska, A. D. Rzoska, and V. Mazur (Springer, Dordrecht, Netherlands, 2010), p. 79.
[15]L. C. Pardo, J. Ll. Tamarit, N. Veglio, F. J. Bermejo, and G. J. Cuello, Phys. Rev. B **76**, 134203 (2007).
[16]M. Rovira-Esteva, N. A. Murugan, L. C. Pardo, S. Busch, J. Ll. Tamarit, Sz. Pothoczki, G. J. Cuello, and F. J. Bermejo, Phys. Rev. B **84**, 064202 (2011).
[17]M. Rovira-Esteva, A. Murugan, L. C. Pardo, S. Busch, M. D. Ruiz-Martín, M. S. Appavou, J. Ll. Tamarit, C. Smuda, T. Unruh, F. J. Bermejo, G. J. Cuello, and S. J. Rzoska, Phys. Rev. B **81**, 092202 (2010).
[18]B. Parat, L. C. Pardo, M. Barrio, J. Ll. Tamarit, P. Negrier, J. Salud, D. O. Lopez, and D. Mondieig, Chem. Mater. **17**, 3359 (2005).
[19]L. C. Pardo, M. Barrio, J. Ll. Tamarit, D. O. Lopez, J. Salud, and H. A. J. Oonk, Chem. Mater. **17**, 6146 (2005).
[20]M. Barrio, J. Ll. Tamarit, Ph. Negrier, L. C. Pardo, N. Veglio, and D. Mondieig, New J. Chem. **32**, 232 (2008).
[21]M. Barrio, P. Negrier, J. Ll. Tamarit, L. C. Pardo, and D. Mondieig, J. Phys. Chem. B **111**, 8899 (2007).
[22]A. H. Narten, M. D. Danford, and H. A. Levy, J. Chem. Phys. **46**, 4875 (1967).
[23]P. A. Egelstaff, D. I. Page, and J. G. Powles, Mol. Phys. **20**, 881 (1971).
[24]P. Jedlovszky, J. Chem. Phys. **107**, 7433 (1997).
[25]P. Jóvári, G. Mészáros, L. Pusztai, and E. Sváb, J. Chem. Phys. **114**, 8082 (2001).
[26]R. Rey, J. Chem. Phys. **126**, 164506 (2007).
[27]Sz. Pothoczki, L. Temleitner, P. Jóvári, S. Kohara, and L. Pusztai, J. Chem. Phys. **130**, 064503 (2009).
[28]M. Howe, R. L. McGreevy, and P. Zetterström, Computer Code CORRECT, Correction Program for Neutron Diffraction Data (NFL Studsvik internal report 1996).
[29]G. Evrard and L. Pusztai, J. Phys. Condens. Matter **17**, S1 (2005).
[30]O. Gereben, P. Jóvári, L. Temleitner, and L. Pusztai, J. Optoel. Adv. Mater. **9**, 3021 (2007).
[31]L. Pusztai and R. L. MecGreevy, J. Chem Phys. **125**, 044508 (2006).
[32]L. Temleitner and L. Pusztai, Phys. Rev. B **81**, 134101 (2010).
[33]L. C. Pardo, M. Rovira-Esteva, S. Busch, M. D. Ruiz-Martin, and J. Ll. Tamarit, J. Phys. Conf. Series J. Phys.: Conf. Ser. **325**, 012006 (2011); L. C. Pardo, M. Rovira-Esteva, S. Busch, J. -F. Moulin, and J. Ll. Tamarit, Phys. Rev. E **84**, 046711 (2011).
[34]J. P. Ryckaert, G. Ciccotti, and H. J. C. Berendsen, J. Comput. Phys. **23**, 327 (1977).